Advances with vertical epitaxial heterostructure architecture (VEHSA) phototransducers for optical to electrical power conversion efficiencies exceeding 50 percent

S. Fafard*[a,b,e], F. Proulx[a,b], M.C.A. York[b], M. Wilkins[c], C. E. Valdivia[c], M. Bajcsy[d], D. Ban[d], A. Jaouad[b], B. Bouzazi[b], R. Arès[b], V. Aimez[b], K. Hinzer[c], D. P. Masson[a],

[a] Azastra Opto Inc., 1420 Blair Place, Suite 601, Ottawa, ON, Canada

[b] Laboratoire Nanotechnologies Nanosystèmes (LN2) – CNRS UMI-3463, Institut Interdisciplinaire d'Innovation Technologique (3IT), Université de Sherbrooke, QC, Canada

[c] Dept. of Electrical Engineering and Computer Science, University of Ottawa, ON, Canada.

[d] Dept. Electrical & Computer Engineering, University of Waterloo, ON, Canada

[e] Department of Physics, University of Ottawa, ON, Canada.

ABSTRACT

A monolithic compound semiconductor phototransducer optimized for narrow-band light sources was designed for and has achieved conversion efficiencies exceeding 50%. The III-V heterostructure was grown by MOCVD, based on the vertical stacking of a number of partially absorbing GaAs n/p junctions connected in series with tunnel junctions. The thicknesses of the p-type base layers of the diodes were engineered for optimal absorption and current matching for an optical input with wavelengths centered in the 830 nm to 850 nm range. The device architecture allows for improved open-circuit voltage in the individual base segments due to efficient carrier extraction while simultaneously maintaining a complete absorption of the input photons with no need for complicated fabrication processes or reflecting layers. Progress for device outputs achieving in excess of 12 V is reviewed in this study.

Keywords: Phototransducer, photovoltaic, power conversion, record efficiencies, VEHSA heterostructure designs, GaAs, MOCVD epitaxy, quantum efficiency.

1. INTRODUCTION

It has been recently demonstrated that the Vertical Epitaxial HeteroStructure Architecture (VEHSA) design is capable of producing phototransducer devices with record optical to electrical conversion efficiencies [1-6]. By vertically stacking a number of partially absorbing GaAs photovoltaic p/n junctions, the output voltage of the resulting phototransducer heterostructure can be readily tailored in steps of about 1.2V per p/n junction. For example, such devices are now commercialized with VEHSA designs built for different applications with a stack of 5, 6, 8, and 12 p/n junctions, referred to as PT5, PT6, PT8, and PT12 devices respectively [2-3]. Modeling of the PT*n* devices has shown that the VEHSA structures are expected to yield optical to electrical conversion efficiencies reaching a remarkable 70% for input powers up to a few watts. Efficiencies around 70% have also already been confirmed experimentally for the PT5 devices [2]. In this study, we review the parameters influencing the conversion efficiency, mainly the temperature, input powers, and input wavelength. In this study we also report on the highest optical efficiencies ever measured for PT12 devices. The details of the structure design used for the study and of the particular applications for phototransducer devices have been published previously [1].

2. EXPERIMENTAL RESULTS

2.1 Spectral response

The VEHSA structures need to be designed for a specific wavelength. The quantum efficiency measurements therefore reveal a response peaking at the design wavelength, around which wavelength the PT*n* devices will operate with the highest efficiency. This is shown in Figure 1. The external quantum efficiency (EQE) measurements are typically obtained at very low optical input powers (in the μW to mW range). Such EQE measurements are shown as symbols in Figure 1 for PT6 and PT8 devices. In additional to the low optical input powers EQE measurements, we measured the device response using the laser output of a tunable Ti:sapphire laser. Using this technique it is possible to verify the spectral response of the PT*n* devices with over 1 W of electrical output power. It is clear from Figure 1 that the higher input power measurements follow closely the EQE measurements obtained at low power. These measurements show that the response of the PT6 device peaks near 820 nm, and the PT8 device near 845 nm. These values are within about 5 nm from the respective design wavelengths.

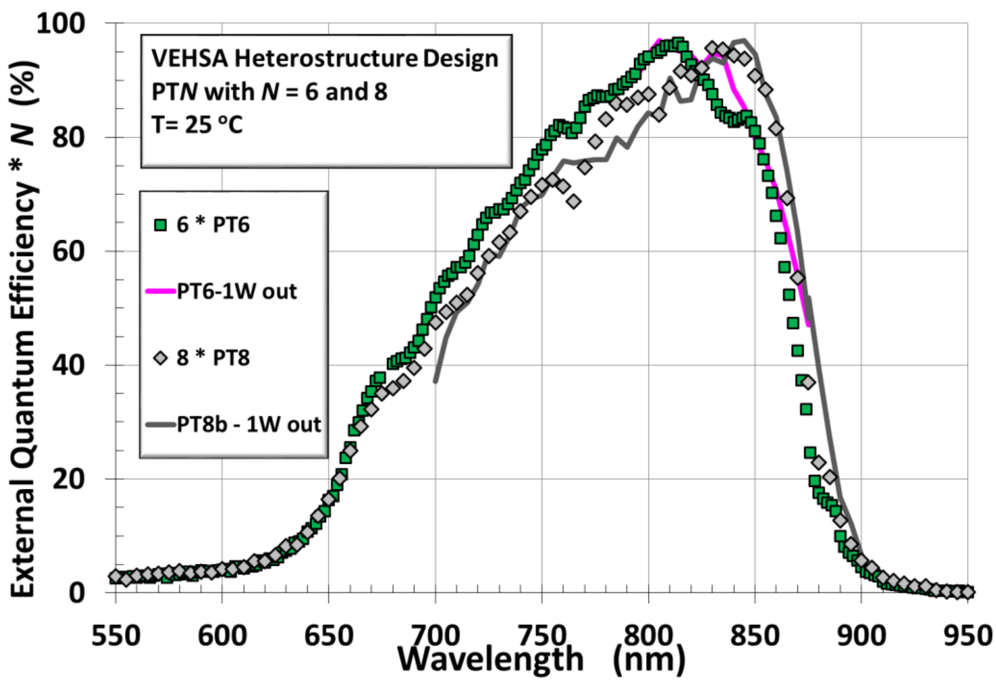

Figure 1. Spectral response of PT6 and PT8 devices. The data with the symbols is obtained at very low power using a standard quantum efficiency (QE) system, whereas the solid lines are measured with greater than 1 W of electrical output with a CW tunable Ti:sapphire laser. The high power measurements have been normalized to obtain the peak value at the same level as the QE data.

2.2 Temperature dependence

The temperature parameters have been previously measured for PT5 devices, with an open-circuit voltage (V_{oc}) reduction of about -7.3 mV/ºC at 1 W input power and -6.4 mV/ºC at 2 W input powers [1]. For PT*n* device with a larger *n*, it is expected that the temperature dependence values will increase with the number of p/n junctions. An example of the temperature-dependent efficiency, V_{oc}, short-circuit current (I_{sc}) and fill factor (*FF*) for the PT6 devices is shown in Figures 2-5. These measurements were obtained with a 3 W optical input power slightly detuned from the peak efficiency. From Figure 2, an efficiency reduction of about 0.05%(abs)/ºC is found for the PT6. The V_{oc} reduction at 3 W for the PT6 is found to be about -7.3 mV/ºC from Figure 3. This is a little higher but consistent with the values obtained for the PT5 when considering that 6 p/n junctions were used instead of 5. Indeed, using the PT5 data at 2 W and a linear relationship with the number of p/n junctions, one would expect a V_{oc} reduction of -6.4/5×6 = -7.7 mV/ºC at 2 W for the PT6. The measured -7.3 mV/ºC is lower because the data was obtained at 3 W instead of 2 W and the V_{oc} reduction decreases with increasing powers. As shown in Figure 4, the I_{sc} is flatter with temperature and decreases with a smaller slope. As can be observed in Figure 5, the *FF* here increases with T. However it should be noted that the exact behavior of the I_{sc} and *FF* is expected to depend significantly on the exciting wavelength and its position with respect to the peak response of the PT*n* device under investigation, as shown in Figure 1.

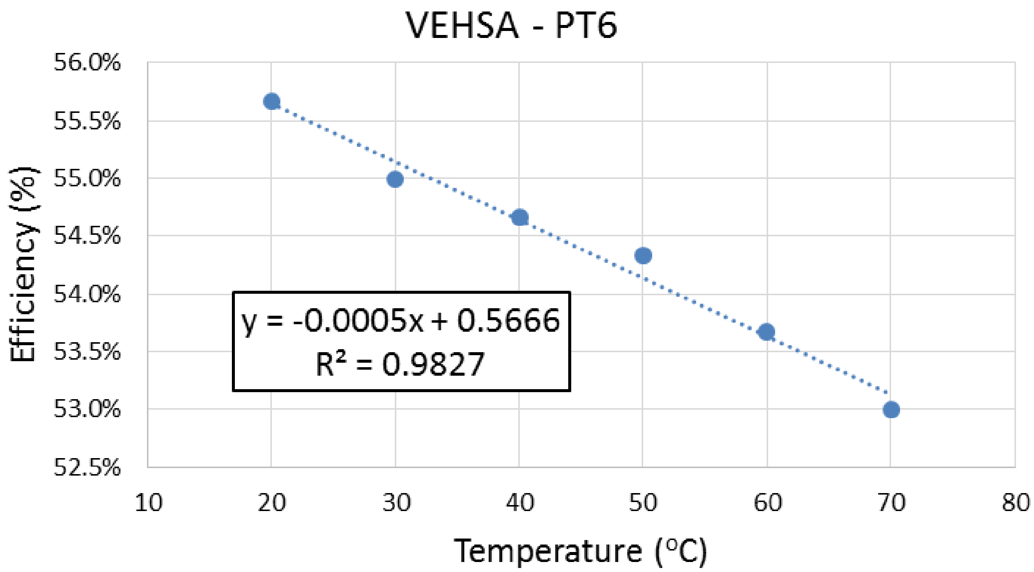

Figure 2. Temperature dependence for a PT6 device measured at 3 W optical input, showing the measured efficiency dependence.

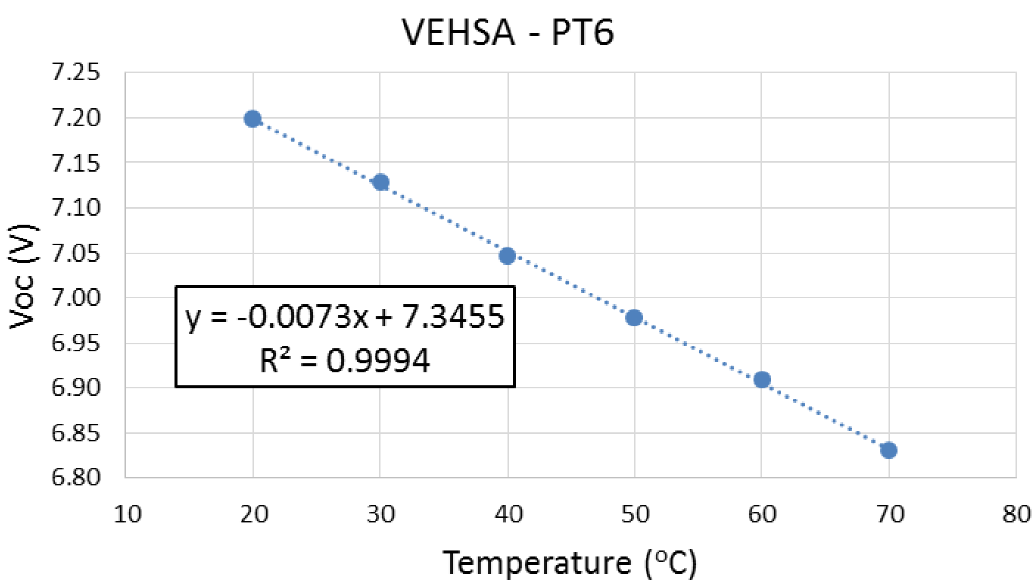

Figure 3. Temperature dependence for a PT6 device measured at 3 W optical input, showing the measured open circuit voltage (V_{oc}) dependence.

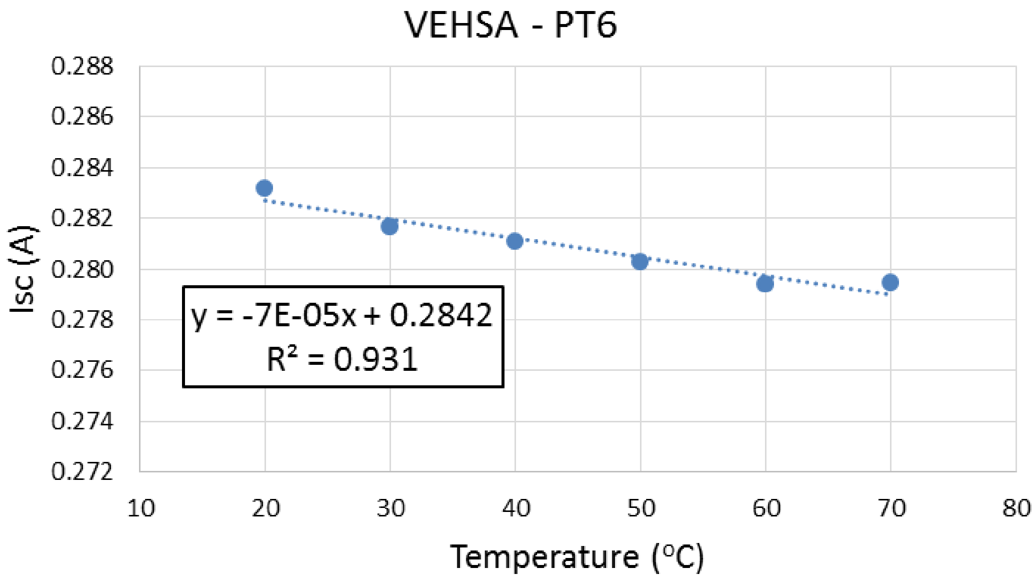

Figure 4. Temperature dependence for a PT6 device measured at 3W optical input, showing the measured short circuit current (I_{sc}) dependence.

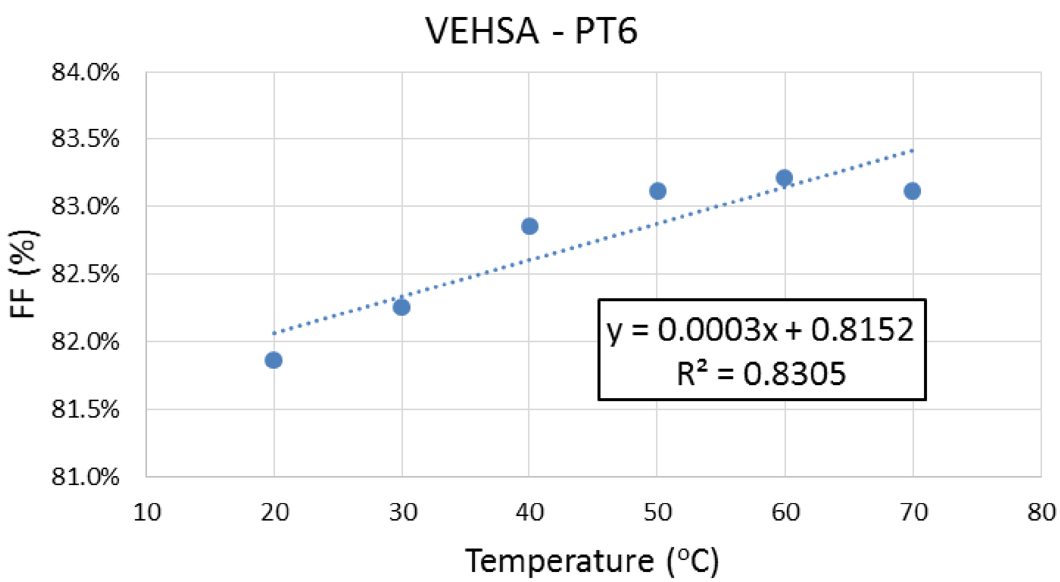

Figure 5. Temperature dependence for a PT6 device measured at 3W optical input, showing the measured fill-factor (*FF*) dependence.

2.3 High-output power operation

The VESHA devices are capable of high efficiencies at high input powers. It is therefore interesting to measure the performance robustness with extended CW operations under high input power conditions. Figure 6 shows the *I-V* data obtained at 4 W input power compared after 5 minutes of continuous operations and after 5 hours. It is clear from the data of Figure 6 that the VEHSA devices have stable performance for extended periods of times while outputting a few watts of electrical power. To further characterize the behavior for longer time periods, Figure 7 shows the time dependence of the performance of a PT6 device for up to 100 hours of continuous operation.

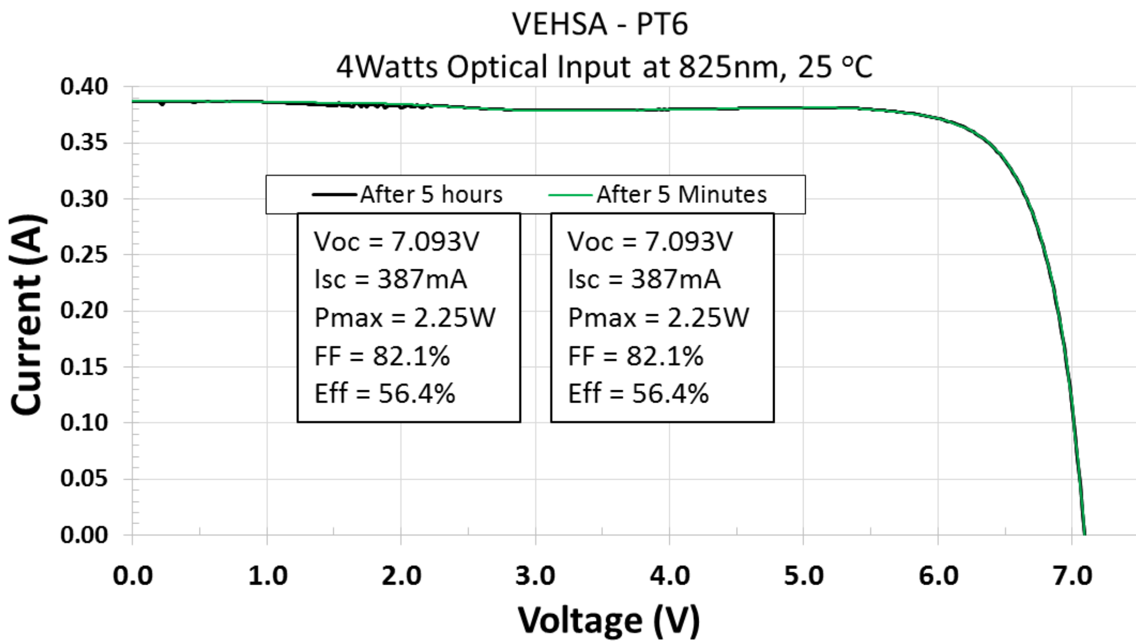

Figure 6. *I-V* data obtained on a new device operated continuously at 4 W of optical input power for 5 minutes compared to 5 hours of continuous operation.

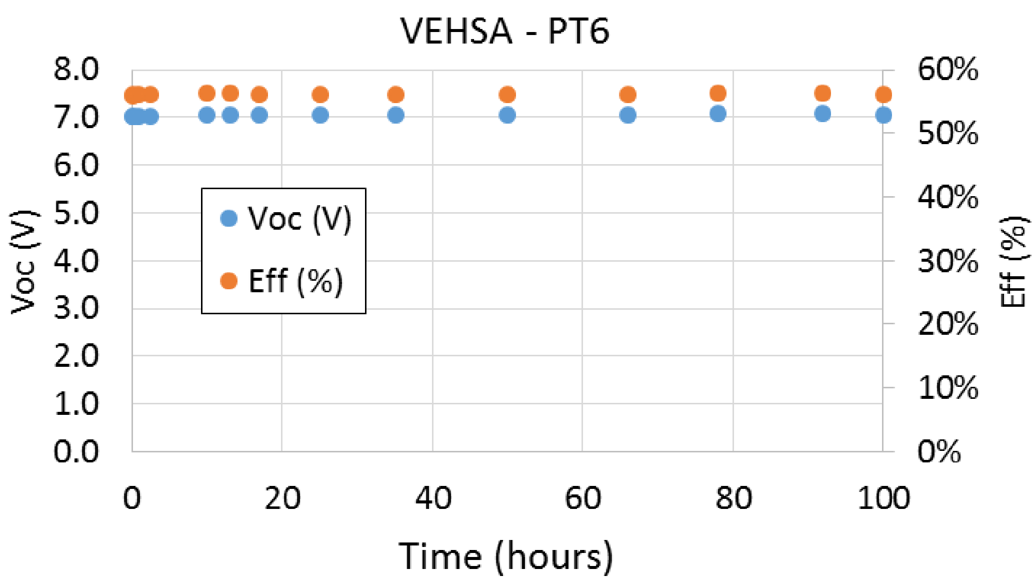

Figure 7. Time dependence of the performance of a PT6 device for 100 hours of continuous operation with an input power of 4 W. The V_{oc} and the efficiency are unaffected (left and right axes, respectively), similarly the I_{sc} and the *FF* remained constant (not shown) with values as per Figure 6 within about 1% relative and therefore within the experimental error.

As seen in Figure 7, the V_{oc}, efficiency (Eff), I_{sc}, *FF* remained unaffected for extended operating times. The values stayed within about 1% relative of the average values throughout the 100 hours of operation at 4 W. This is therefore within the experimental error of such measurements.

2.4 VEHSA devices with higher voltages

The PT8 and PT12 devices have also been shown to be capable of >50% conversion efficiencies with a few watt of electrical output power [2]. However, to date the efficiencies obtained with the PT8 or PT12 devices are smaller than both the 70% predicted from computer modeling and the values measured with the PT5 devices. The main factor responsible for the lower efficiency has been associated with the de-tuning of the test laser from the peak efficiency as per Figure 1. To evaluate the performance of the PT12 devices under more favorable conditions closer to the designed optimal wavelength, we here present results obtained with a high-power laser diode having an output wavelength at ~850 nm. The output at 850 nm is less detuned from the peak response of our PT8 and PT12 VEHSA design. Also to minimize the performance degradation with temperature, the efficiency measurements in Figure 8 were taken shortly after turning on the laser diode to avoid a temperature increase of the junctions under operation. The efficiencies obtained at 850 nm are 60.9% and 60.3% for the PT8 and PT12, respectively. A maximum V_{oc} value of 14.67 V was thus obtained with the PT12 device at an input power of 4.4 W. A V_{oc} value of 9.71 V was obtained with the PT8 device at an input power of 1.8 W. The measured V_{oc} values are slightly higher than the modeled values. For example, from the model we would expect for the PT12 VEHSA structure 14.6 V at 5 W. Similarly from the model we would expect for the PT8 VEHSA structure 9.55 V at 1.7 W [2]. We previously observed, however, that the exact values of the V_{oc} predicted from the modeling can depend on the details of the material parameters chosen, particularly for the bandgap narrowing and the lifetime values.

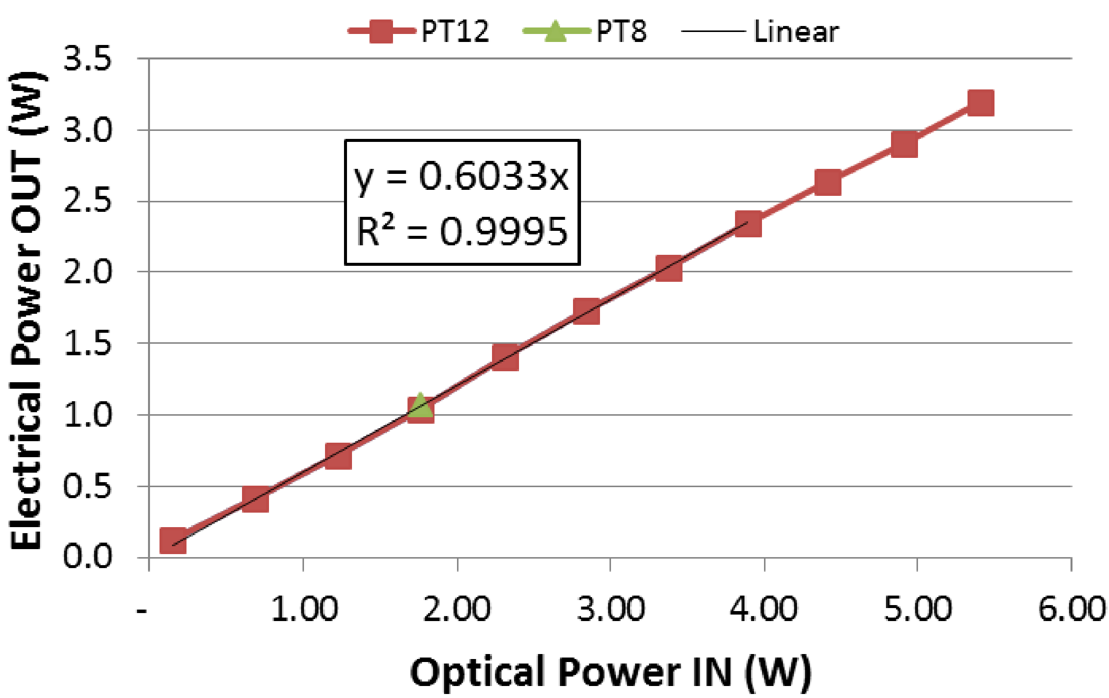

Figure 8. Efficiency measurements for PT8 and PT12 VEHSA devices excited with a high-power laser diode at 850 nm. The efficiencies are best obtained directly from the slope of the Power IN vs Power OUT linear fit given the strong correlation factor measured. The efficiencies obtained at that wavelength are 60.9% and 60.3% for the PT8 and PT12, respectively. Only one point is displayed for PT8, but it yields very similar measured values as the PT12 device.

2.5 Opto-coupler performance

Given the record performance of the VEHSA phototransducers, it is interesting to study the performance of opto-coupler (OC) devices built by integrating a high-power laser diode with a PT*n* device. Using a straight forward geometry, the laser diode and a PT*n* device were arranged in a face-to-face configuration with an air gap of about 1 mm between them to providing full isolation. The geometry was not optimized for these initial tests, and a small fraction of the laser output beam may not have been perfectly matched to the phototransducer active area. On the other hand,, the wavelength tuning is close to ideal for the PT8 and PT12 devices and high optical-to-electrical (O-E) and electrical-to-electrical (E-E) efficiencies are seen, as shown in Table 1. The maximum opto-coupler E-E is about 26% for an opto-coupler electrical output between about 1.7 W and 2.6 W. The opto-coupler based on the PT8 phototransducers provides similar performance. The PT6 phototransducers used here are tuned for about 820 nm and are therefore detuned for operation at 850 nm. The opto-coupler based on the PT6 phototransducers are therefore giving an E-E performance a little bit more than a relative 10% lower than when using a tuned PT*n* device.

Table 1. Opto-coupler (OC) performance obtained in face-to-face configuration of an 850 nm laser diode and various PT*n* phototransducers.

VEHSA type	Laser Current	Laser Voltage	Laser Output Power	Laser Eff	PT's Voc	PT's Isc	PT's Pmax	PT's O-E Eff	OC's E-E Eff
	A	V	W	%	V	mA	W	%	%
PT12	1.0	1.63	0.15	9.1	13.49	10	0.12		7.3%
PT12	1.5	1.68	0.68	27.1	14.14	33	0.42	61.1%	16.6%
PT12	2.0	1.74	1.22	35.0	14.34	57	0.72	58.9%	20.6%
PT12	2.5	1.80	1.76	39.3	14.47	82	1.04	59.1%	23.2%
PT12	3.0	1.85	2.31	41.6	14.54	109	1.40	60.9%	25.3%
PT12	3.5	1.90	2.84	42.7	14.57	134	1.73	60.8%	26.0%
PT12	4.0	1.95	3.37	43.2	14.62	157	2.03	60.2%	26.0%
PT12	4.5	2.00	3.89	43.2	14.66	180	2.35	60.4%	26.1%
PT12	5.0	2.05	4.41	43.1	14.67	206	2.64	59.8%	25.7%
PT12	5.5	2.10	4.91	42.6	14.65	225	2.91	59.2%	25.2%
PT12	6.0	2.14	5.40	42.1	14.63	247	3.19	59.0%	24.8%
PT8	2.5	1.80	1.76	39.3	9.71	124	1.07	60.9%	23.9%
PT6 (detuned)	2.5	1.80	1.76	39.3	7.24	154	0.95	53.7%	21.1%

3. CONCLUSIONS

Our study demonstrated that the observed properties of thin n/p heterostructures can be directly exploited in optoelectronic devices based on vertical epitaxial heterostructure architectures (VEHSA) design. The results have been previously exploited in novel high-efficiency PT5 VEHSA devices with record efficiencies. In this study we extended the applications to cover PT6, PT8, and PT12 designs. These breakthrough developments demonstrated that unprecedented 70% conversion efficiencies are achievable with tailored output voltages and with a few watts of electrical output powers. In this study we have demonstrated PT8 and PT12 performance in excess of 60%. To reach the 70% level, wavelength tuning is necessary and can readily be achieved by matching the laser diode output to the PT*n* design or vice versa. We have started to characterize the temperature dependence of the PT*n* device. Proper thermal management of the PT*n* devices is important to achieve the highest efficiencies. The efficiency increases with the optical input powers [2], but if a design with a proper cooling is not used the performance can roll-off with a few watts of optical input powers. The V_{oc} reduction at 3 W for the PT6 was confirmed to be about -7.3 mV/ºC and the V_{oc} reduction for a PT12 device is expected to be about twice that value.

Record performances have been obtained with various PT*n* VEHSA designs. An output voltage of 14.67V has been measured with the PT12 devices around a 2.6 W electrical output, yielding an effective 1.22 V per p/n junctions by using the thin p/n junction in the VEHSA design. An opto-coupler electrical-to-electrical conversion efficiency of 26% was measured for an opto-coupler electrical output between about 1.7 W and 2.6 W.

4. ACKNOWLEDGMENTS

The authors are grateful to the Ministère de l'Économie, de l'Innovation et des Exportations for their financial support. We would also like to thank Azastra Inc for their funding that permitted the genesis of this work, as well as the Industrial Research Assistance Program from the National Research Council of Canada for their financial assistance. KH, CEV, MW would like to acknowledge the support of the Canadian Foundation for Innovation and the Ontario Research Fund for their equipment funding support and scholarships support. KH would like to acknowledge the Canada Research Chair program, and MW would like to acknowledge the Natural Sciences and Engineering Research Council (NSERC) Canada for their scholarship support.

REFERENCES

*simon.fafard@usherbrooke.ca or simon.fafard@azastra.com

[1] D.P. Masson, F. Proulx, and S. Fafard, Prog. Photovolt: Res. Appl. 23, 1687–1696 (2015).
[2] S. Fafard, M. York, V. Aimez, K. Hinzer, F. Proulx, C. E. Valdivia, M. M. Wilkins, R. Arès, and D. P. Masson, Appl. Phys. Lett., in review, 2016.
[3] M.C.A. York, F. Proulx, D. P. Masson, A. Jaouad, B. Bouzazi, R. Arès, V. Aimez, and S. Fafard, MRS Advances, pp 1 - 10, 2015 MRS Fall Meeting Proceedings (2016).
[4] C.E. Valdivia, M.M. Wilkins, B. Boussairi, A. Jaouad, V. Aimez, R. Arès, D.P. Masson, S. Fafard, and K. Hinzer, SPIE OPTO, p. 93580E, International Society for Optics and Photonics (2015).
[5] S. Fafard and D. P. Masson, US Patent App. 61913675 (2013)
[6] Wilkins, M., Valdivia, C.E., Gabr, A.M., Masson, D., Fafard, S., Hinzer, K., J. Appl. Phys. 118-15, (2015).